A Magnetar-Asteroid Impact Model for FRB 200428 Associated with an X-ray Burst from SGR 1935+2154

Zigao Dai

School of Astronomy and Space Science, Nanjing University

Dai 2020, ApJL, 897, L40
Dai & Zhong 2020, ApJL, 895, L1
Dai, Wang, Wu & Huang 2016, ApJ, 829, 27
Liu, Wang, Yang & Dai 2020, ApJ, accepted, arXiv:2010.14379

2nd workshop on GECAM, 31 October – 1 September 2020

A comet-Jupiter impact

16-22 July 1994

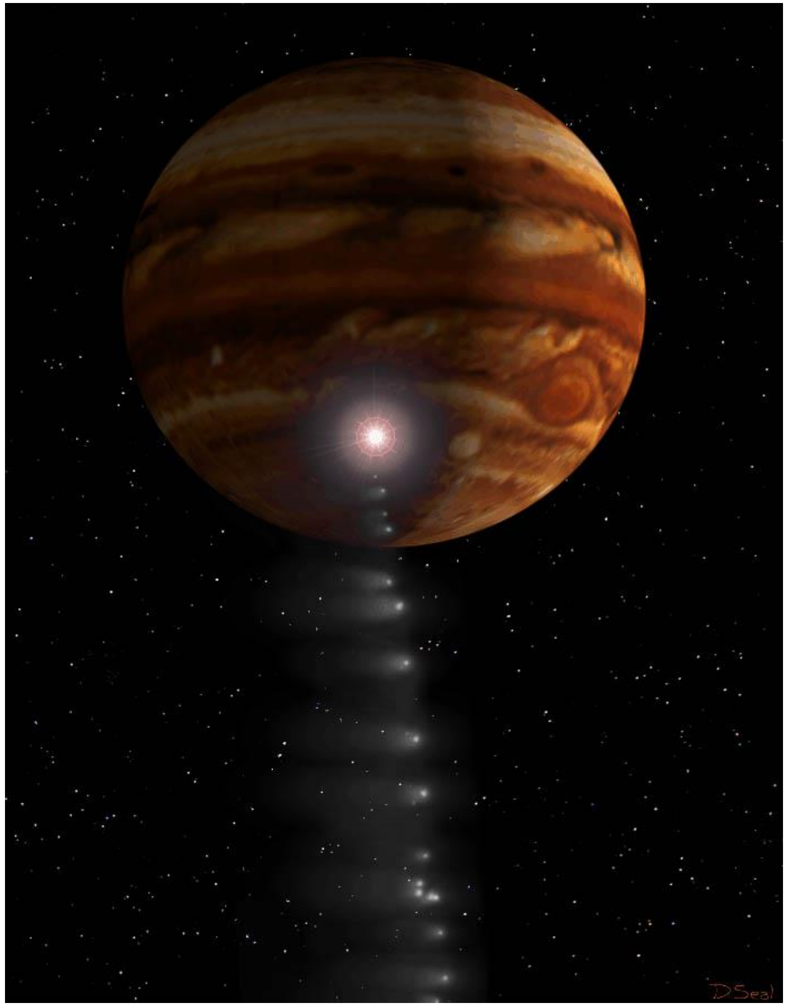

Comet Shoemaker-Levy 9: 21 fragments; **Dinosaur extinction: asteroid-earth impact**

FRB from encounter of a pulsar and an asteroid

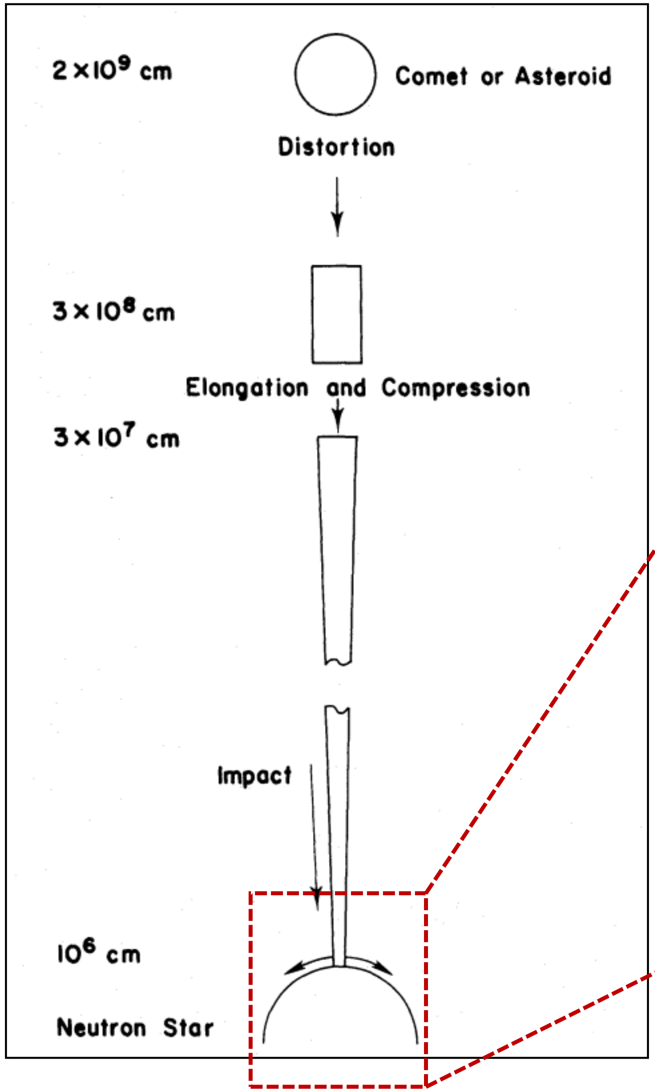

Colgate & Petschek 1981

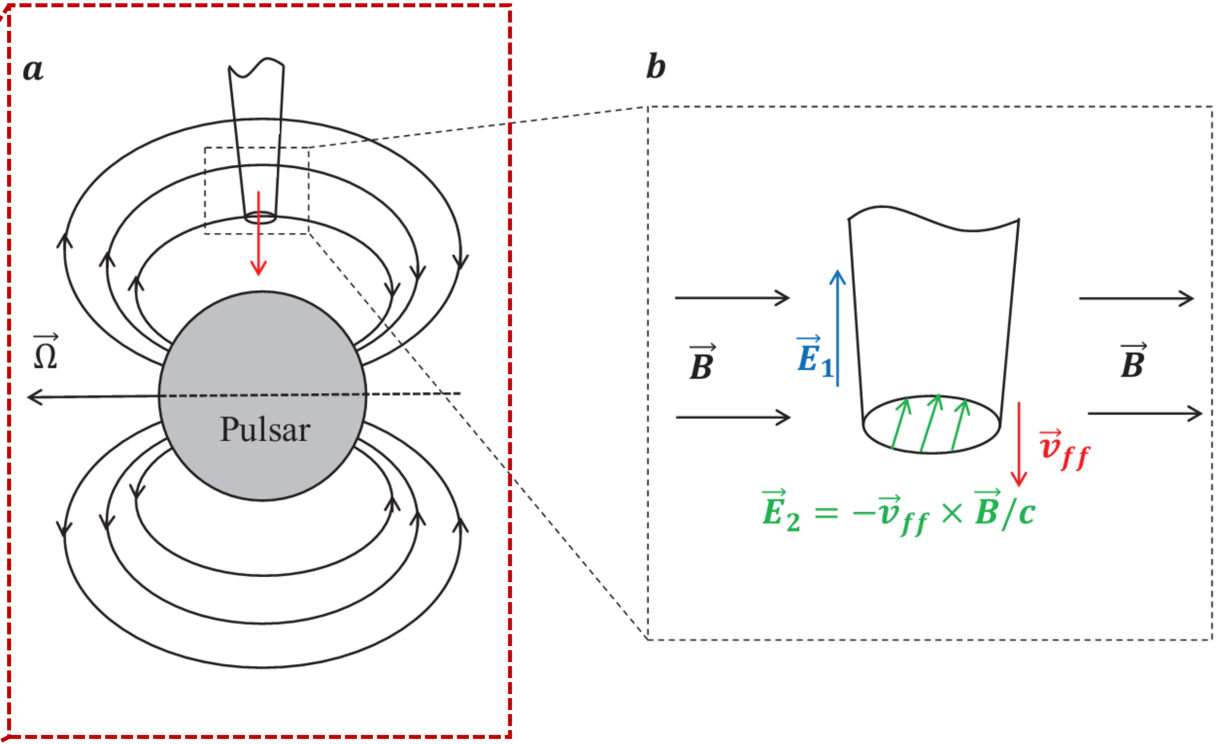

Dai, Wang, Wu & Huang 2016, ApJ, 829, 27

"The belt & road" model: periodicity

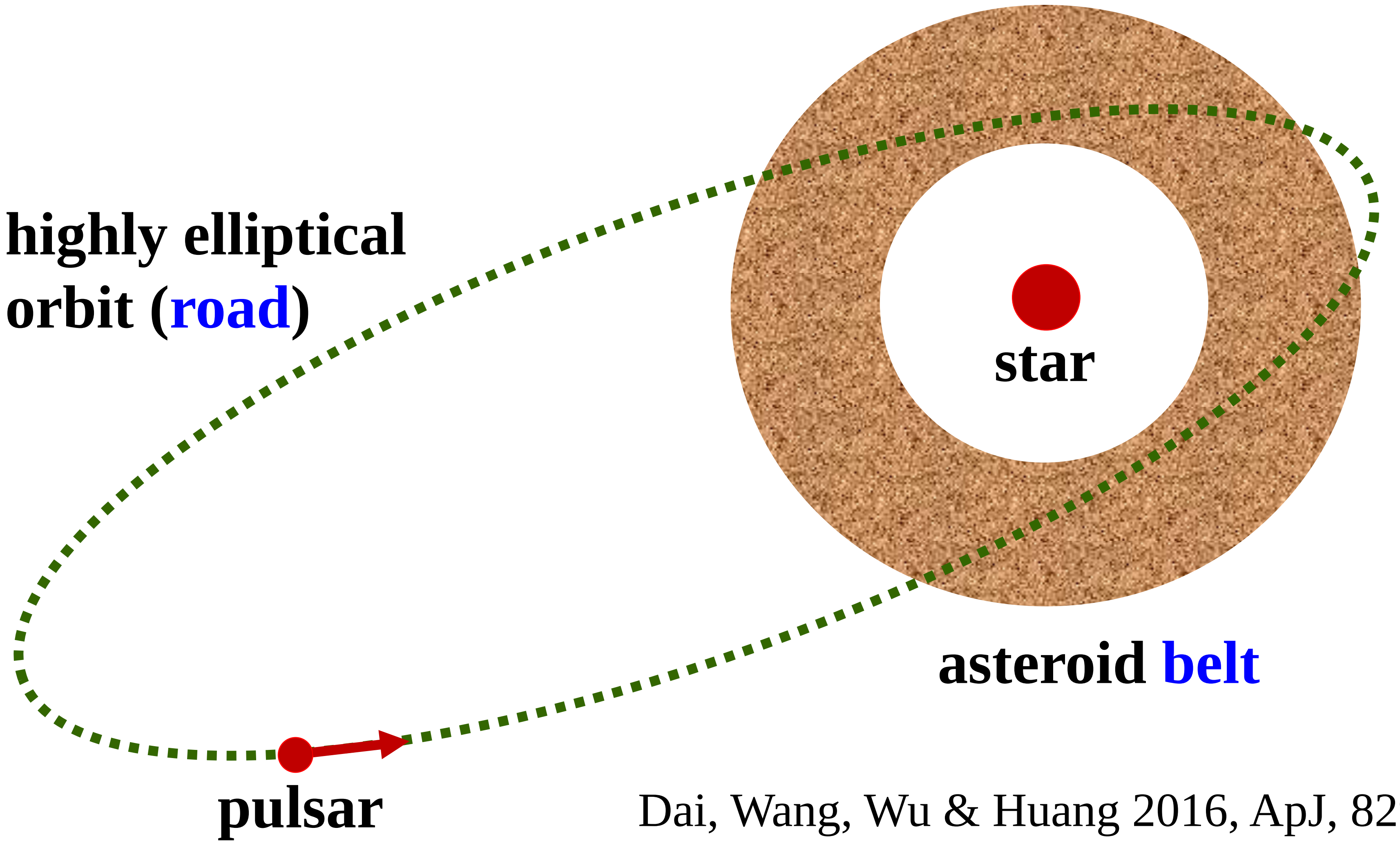

Dai, Wang, Wu & Huang 2016, ApJ, 829, 27
FRB 121102: Bagchi 2017, ApJL, 838, L16

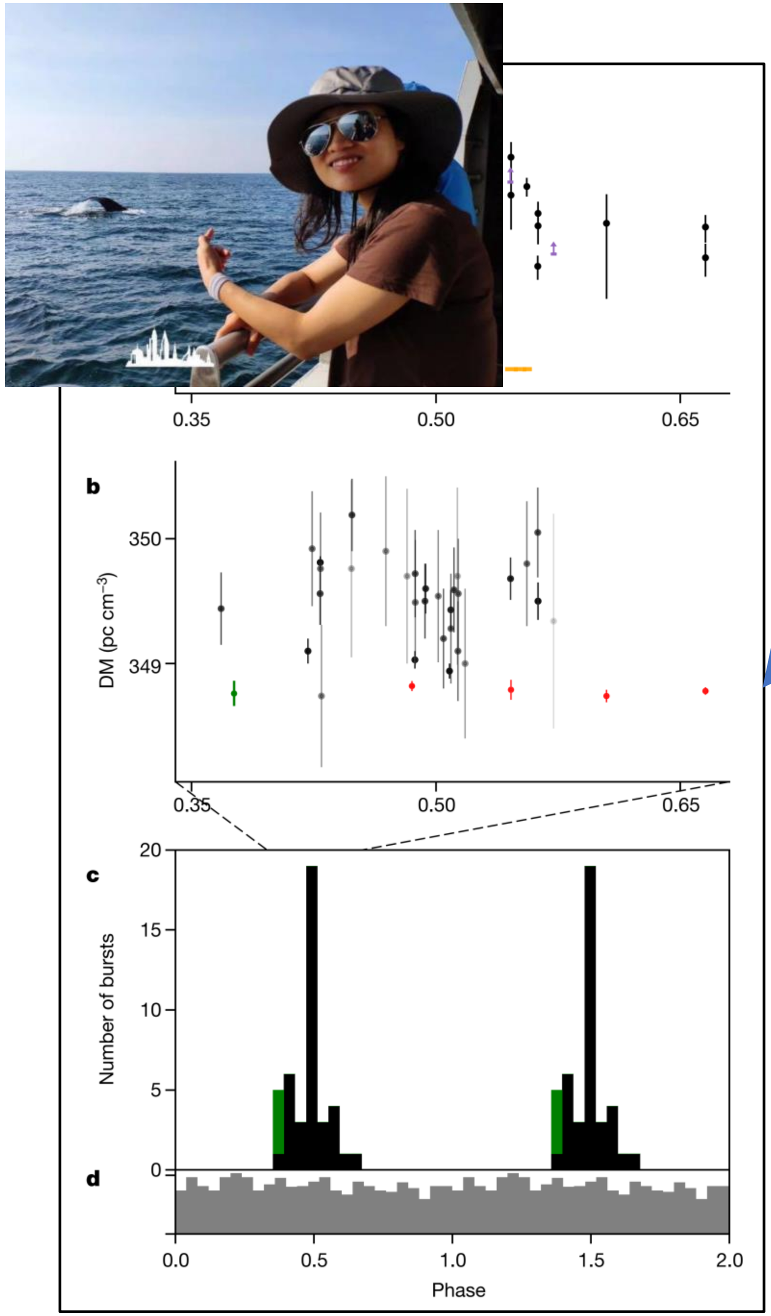

The first light of understanding FRBs

- **Periodic (~16 day) activity from FRB 180916.J0158+65** (CHIME/FRB Collaboration et al. 2020, Nature, 582, 351)
  - **Precessing magnetars** (Yang & Zou 2020; Levin et al. 2020; Zanazzi & Lai 2020)
  - **Strongly magnetized neutron stars in binaries** (Dai & Zhong 2020; Lyutikov et al. 2020; Ioka & Zhang 2020)
- **FRB 200428 and its associated X-ray burst (XRB) from the Galactic magnetar SGR 1935+2154**

The Astrophysical Journal Letters, 895:L1 (6pp), 2020 May 20 https://doi.org/10.3847/2041-8213/ab8f2d

Periodic Fast Radio Bursts as a Probe of Extragalactic Asteroid Belts

Z. G. Dai[1,2] and S. Q. Zhong[1,2]

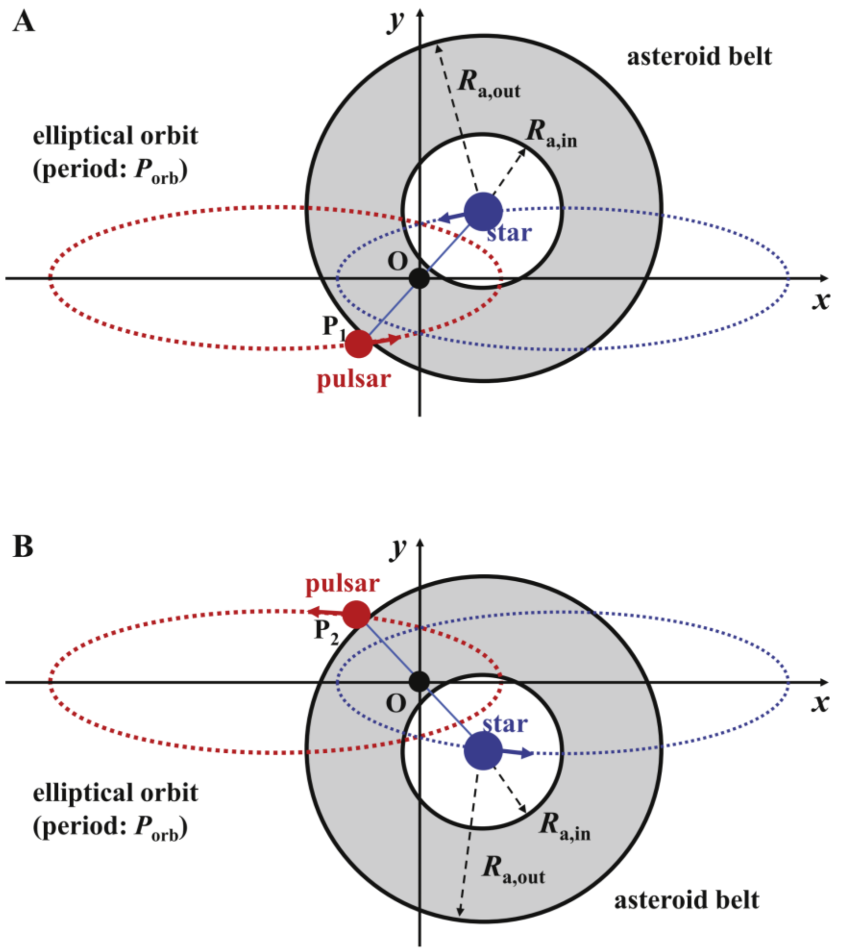

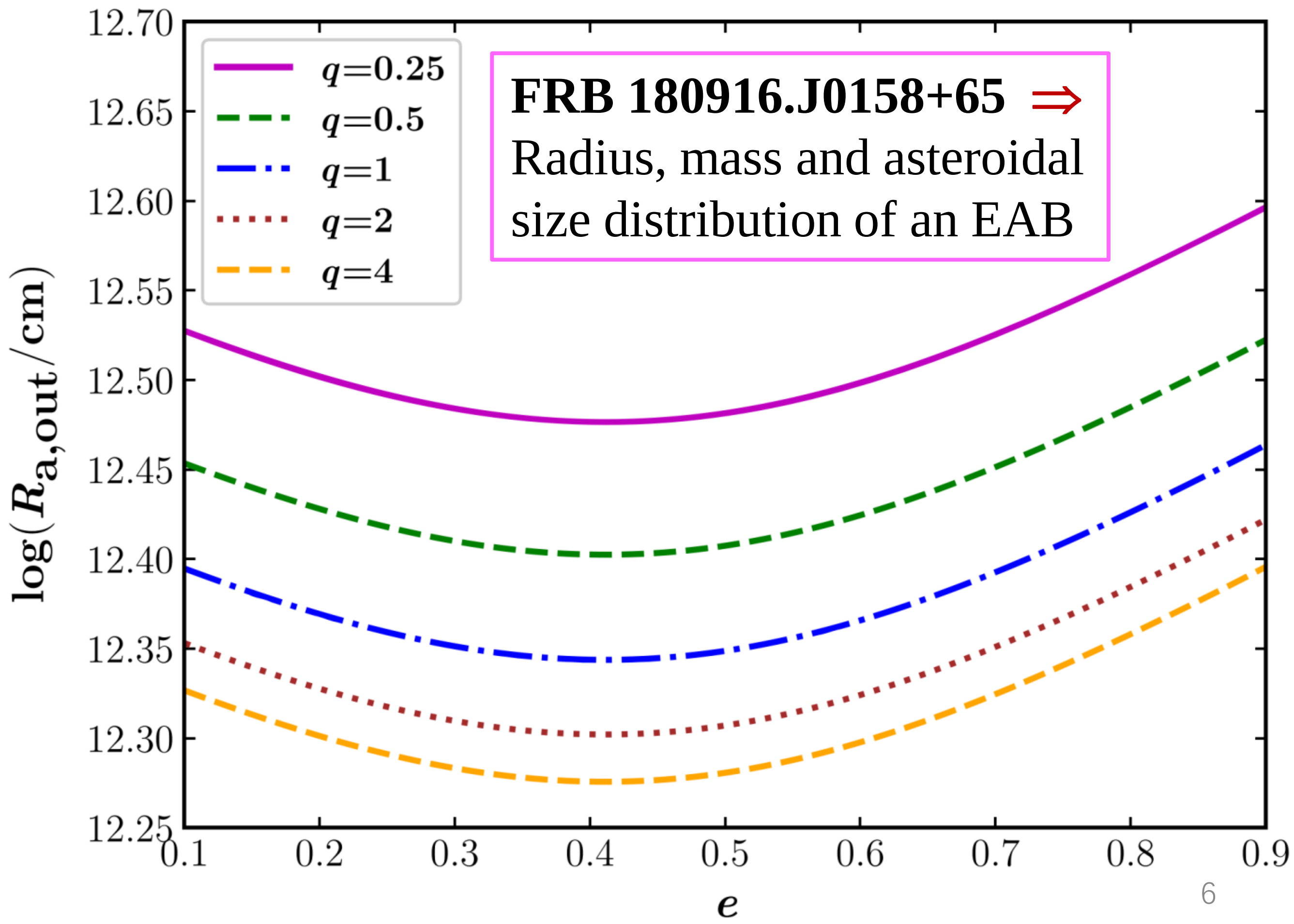

Outline

1. Observed features
2. Magnetar-asteroid impact model
3. Constraints on model parameters
4. Conclusions

1. Observed features

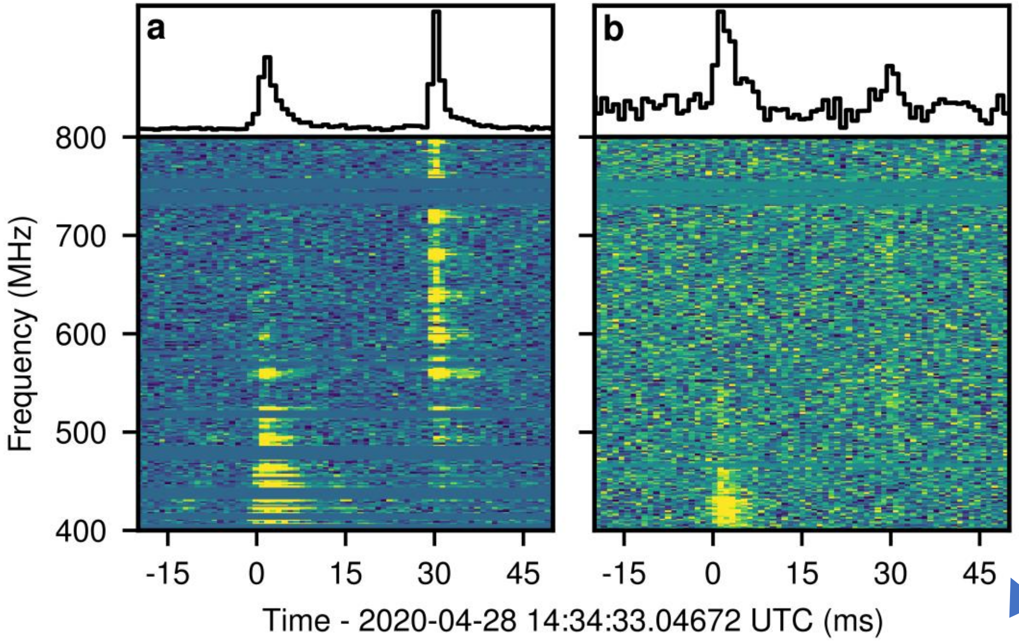

$$E_{\mathrm{CHIME}} = 3^{+3.0}_{-1.6} \times 10^{34}\ \mathrm{erg}$$

$$E_{\mathrm{STARE2}} = (2.2 \pm 0.4) \times 10^{35}\ \mathrm{erg}$$

for the source's distance ***D* ~ 10 kpc**

- **FRB 200428 with two pulses of intrinsic durations ~ 0.60 ms and ~ 0.34 ms from SGR 1935+2154 was reported. The two pulses are separated by ~ 28.91 ms.**
- **This FRB has a fluence of 0.7 MJy ms and 1.5 ± 0.3 MJy ms detected by the CHIME and STARE2 telescopes, respectively.**

CHIME/FRB Collaboration et al. 2020, arXiv:2005.10324
STARE2: Bochenek et al. 2020, arXiv:2005.10828

THE ASTROPHYSICAL JOURNAL LETTERS, 898:L5 (6pp), 2020 July 20 https://doi.org/10.3847/2041-8213/aba262

On the Distance of SGR 1935+2154 Associated with FRB 200428 and Hosted in SNR G57.2+0.8

Shu-Qing Zhong[1,2], Zi-Gao Dai[1,2], Hai-Ming Zhang[1,2], and Can-Min Deng[3,4]

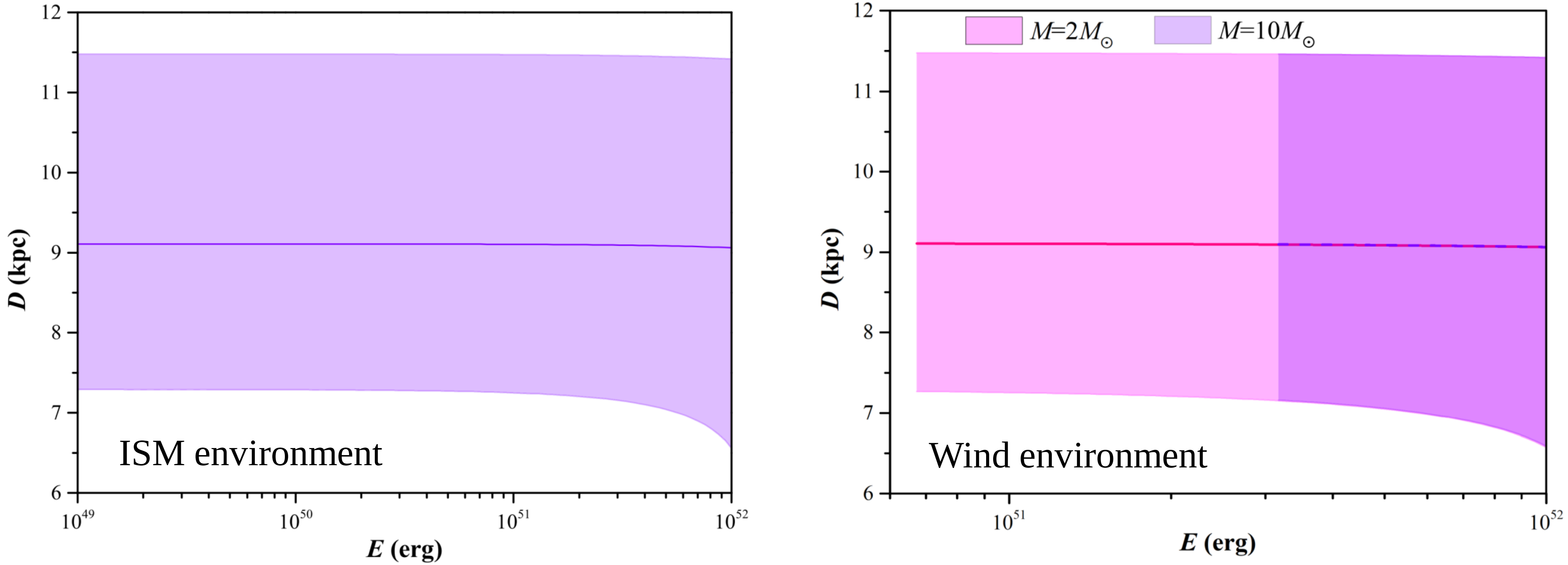

Dispersion Measure and Rotation Measure $\Rightarrow$ $D = 9.0 \pm 2.5$ **kpc**

THE ASTROPHYSICAL JOURNAL, 829:27 (7pp), 2016 September 20 doi:10.3847/0004-637X/829/1/27

Prediction of an XRB

CrossMark

REPEATING FAST RADIO BURSTS FROM HIGHLY MAGNETIZED PULSARS TRAVELING THROUGH ASTEROID BELTS

Z. G. DAI[1,2], J. S. WANG[1,2], X. F. WU[3,4], AND Y. F. HUANG[1,2]

We further discuss the other possible phenomenon in the pulsar-asteroid encounter model. When an asteroid impacts the surface of a pulsar, a resultant hot spot with radius given approximately by Equation (6) is powered by the gravitational energy release, but meanwhile it is cooled down by the surface blackbody radiation. Under the assumption of thermal equilibrium, the temperature of the hot spot is estimated by $T_{\rm spot} \sim (\dot{E}_{\rm G}/\sigma_{\rm SB}\pi r^2)^{1/4} = 1.64 \times 10^9 m_{18}^{1/36} \rho_{0,0.9}^{19/72} s_{10}^{-1/24} (M/1.4M_\odot)^{5/12} R_{*,6}^{-1/2}$ K, where $\sigma_{\rm SB}$ is the Stefan–Boltzmann constant. We see that this blackbody temperature is very weakly dependent on asteroidal mass and that the emission from the hot spot turns out to be at soft gamma-ray energies rather than X-ray energy suggested by Huang & Geng (2014) and Geng & Huang

(2015). This is the reason that pulsar-asteroid impacts were widely argued to be an origin of nearby GRBs in the early literature. Assuming isotropic emission, the farthest distance of such GRBs is estimated by $D_{\rm GRB,max} \sim (\dot{E}_{\rm G}/4\pi F_\gamma)^{1/2} = 31.4 m_{18}^{5/18} \rho_{0,0.9}^{5/36} s_{10}^{1/12} (M/1.4M_\odot)^{2/3} R_{*,6}^{-1/2} F_{\gamma,-12}^{-1/2}$ Mpc, where $F_\gamma = F_{\gamma,-12} \times 10^{-12}$ erg cm^{-2} s^{-1} is the sensitivity of a detector. Further assuming the total rate of FRBs $\mathcal{R}_{\rm FRB} \sim 10^4$ sky^{-1} day^{-1} and their farthest distance $D_{\rm FRB,max} \sim 3.2$ Gpc (Thornton et al. 2013), we obtain the observable rate of GRBs, $\mathcal{R}_{\rm GRB} \sim \mathcal{R}_{\rm FRB} (D_{\rm GRB,max}/D_{\rm FRB,max})^3 \sim 3.44 m_{18}^{5/6} \rho_{0,0.9}^{5/12} s_{10}^{1/4} (M/1.4M_\odot)^2 R_{*,6}^{-3/2} F_{\gamma,-12}^{-3/2}$ yr^{-1}, if all FRBs result from pulsar-asteroid impacts. This implies that only a few extremely low-luminosity GRBs associated with FRBs per year would be detected by a satellite with sensitivity of $F_\gamma = 10^{-12}$ erg cm^{-2} s^{-1}.

Insight-HXMT: Li et al. 2020

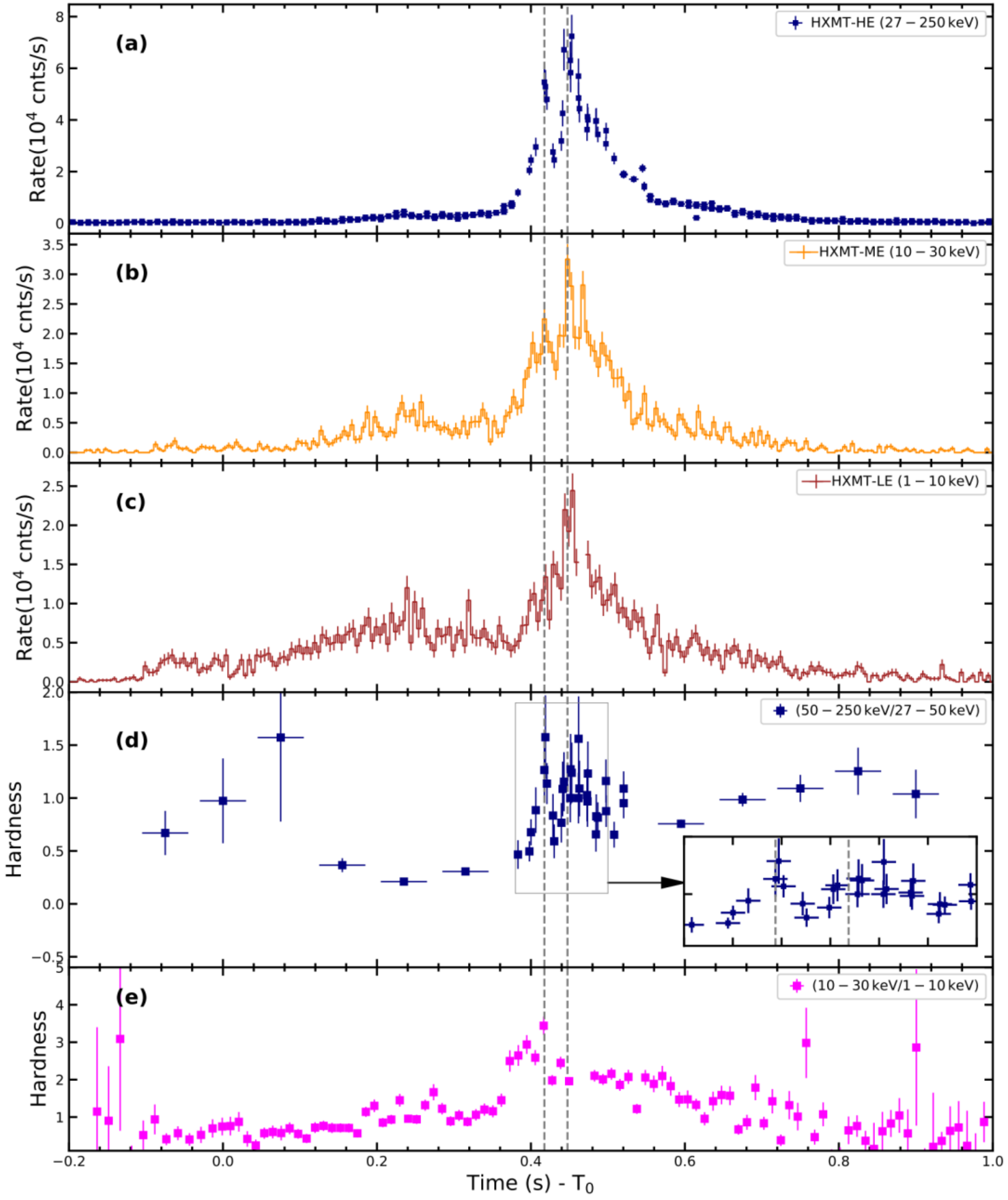

- **An XRB with two peaks associated with FRB 200428 was simultaneously detected by a few high-E satellites.**
- **The XRB's spectrum can be fitted by a cutoff power law (CPL) or two-T BB (kT_1 ~ 11 keV and kT_2 ~ 30 keV) or BB + PL model.**

$$\boxed{E_X \sim (0.8 - 1.2) \times 10^{40} (D/10\,\mathrm{kpc})^2\,\mathrm{erg}}$$

Insight-HXMT: Li et al. 2020, arXiv:2005.11071
INTEGRAL: Mereghetti et al. 2020, arXiv:2005.06335
Konus-Wind: Ridnaia et al. 2020, arXiv:2005.11178
AGILE: Tavani et al. 2020, arXiv:2005.12164

Magnetar-based interior-driven models: Lyutikov & Popov 2020; Margalit+2020; Lu, Kuamr & Zhang 2020

2. The magnetar-asteroid impact model

THE ASTROPHYSICAL JOURNAL LETTERS, 897:L40 (6pp), 2020 July 10 https://doi.org/10.3847/2041-8213/aba11b

CrossMark

A Magnetar-asteroid Impact Model for FRB 200428 Associated with an X-Ray Burst from SGR 1935+2154

Z. G. Dai[1,2]

- **Assumption: an old-aged magnetar encounters an asteroid of mass $m_a \sim 10^{20}$ g.**
- **Physically, this asteroid is first disrupted tidally into a great deal of fragments, and then two major iron-nickel fragments of $m \sim 10^{17}$ g are distorted.**

THE ASTROPHYSICAL JOURNAL LETTERS, 898:L55 (6pp), 2020 August 1 https://doi.org/10.3847/2041-8213/aba83c

(1) XRB， (2) FRB

CrossMark

FRB 200428: An Impact between an Asteroid and a Magnetar

Jin-Jun Geng[1,2], Bing Li[3,4], Long-Biao Li[5,6], Shao-Lin Xiong[3], Rolf Kuiper[2], and Yong-Feng Huang[1,6]

Disruption radius: $R_\mathrm{d} \sim (M/m_\mathrm{a})^{1/3} r_\mathrm{a} \sim 6.1 \times 10^{10} (M/1.4M_\odot)^{1/3}\,\mathrm{cm}$

Fragmental breakup radius: $R_\mathrm{b} = 1.3 \times 10^{9} (m/10^{17}\,\mathrm{g})^{2/9} (M/1.4M_\odot)^{1/3}\,\mathrm{cm}$

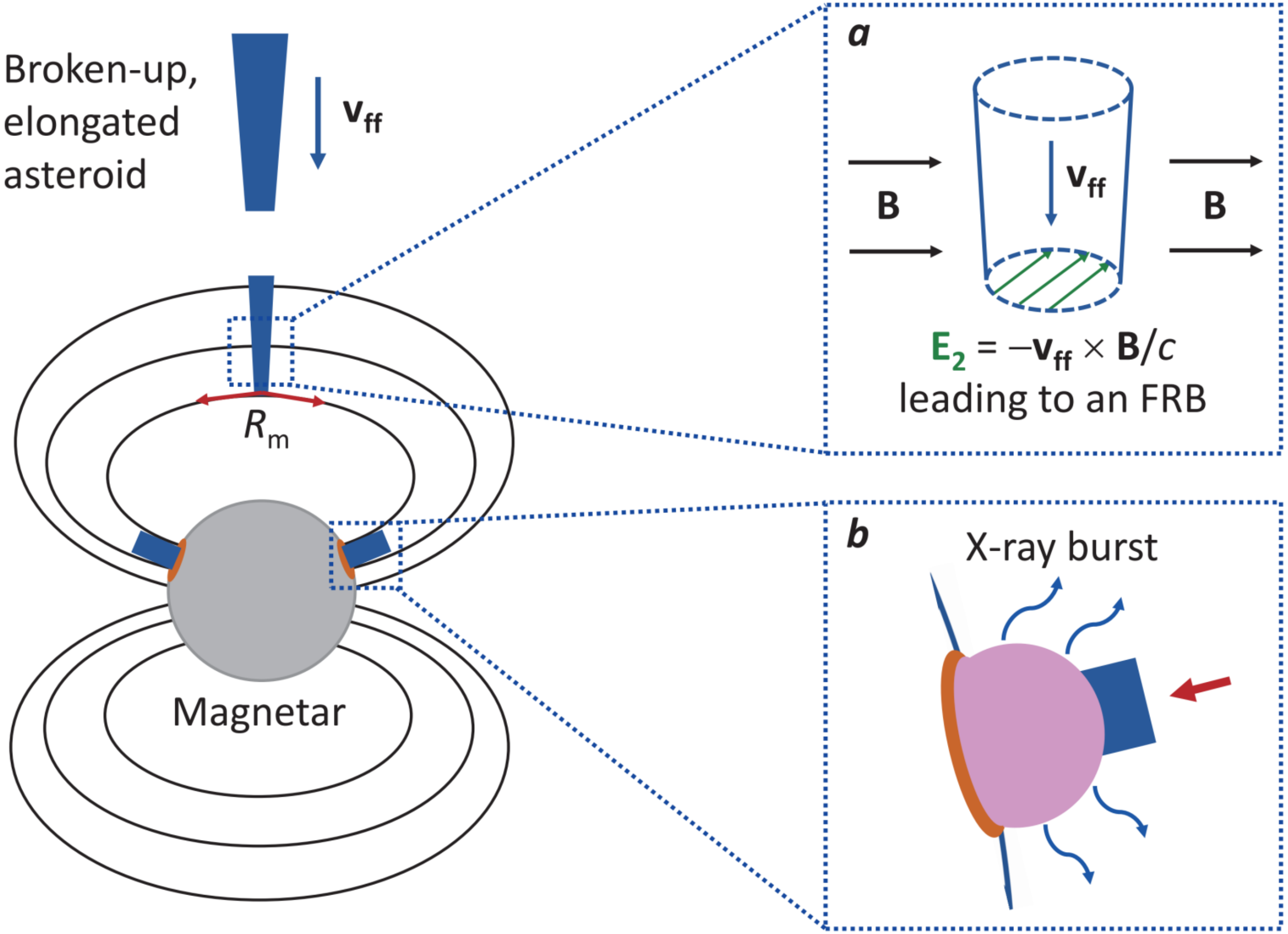

Dai 2020, ApJL, 897, L40

The accretion duration of a major fragment (Dai et al. 2016, ApJ, 829, 27):

$$\Delta t \simeq \frac{12 r_0}{5} \left(\frac{R_\mathrm{b}}{GM} \right)^{1/2} = 0.57 \left(\frac{m}{10^{17}\,\mathrm{g}} \right)^{4/9} \left(\frac{M}{1.4 M_\odot} \right)^{-1/3} \mathrm{ms}$$

For the first pulse ($\Delta t \approx 0.6$ ms) of FRB 200428, the fragmental mass:

$$m \simeq 1.1 \times 10^{17} \left(\frac{\Delta t}{0.6\,\mathrm{ms}} \right)^{9/4} \left(\frac{M}{1.4 M_\odot} \right)^{3/4} \mathrm{g}$$

The magnetic interaction radius (≈ the Alfven radius):

$$R_\mathrm{m} \simeq 1.2 \times 10^{7} \left(\frac{\Delta t}{0.6\,\mathrm{ms}} \right)^{-1/18} \left(\frac{M}{1.4 M_\odot} \right)^{-15/54} \left(\frac{\mu}{2.2 \times 10^{32}\,\mathrm{G\,cm^3}} \right)^{4/9} \mathrm{cm}$$

The radius of this elongated cylindrical fragment at R_m:

$$r(R_\mathrm{m}) \simeq 2.1 \times 10^{4} \left(\frac{\Delta t}{0.6\,\mathrm{ms}} \right)^{17/36} \left(\frac{M}{1.4 M_\odot} \right)^{-15/108} \left(\frac{\mu}{2.2 \times 10^{32}\,\mathrm{G\,cm^3}} \right)^{2/9} \mathrm{cm}$$

Geometry of an FRB-Emitting Region

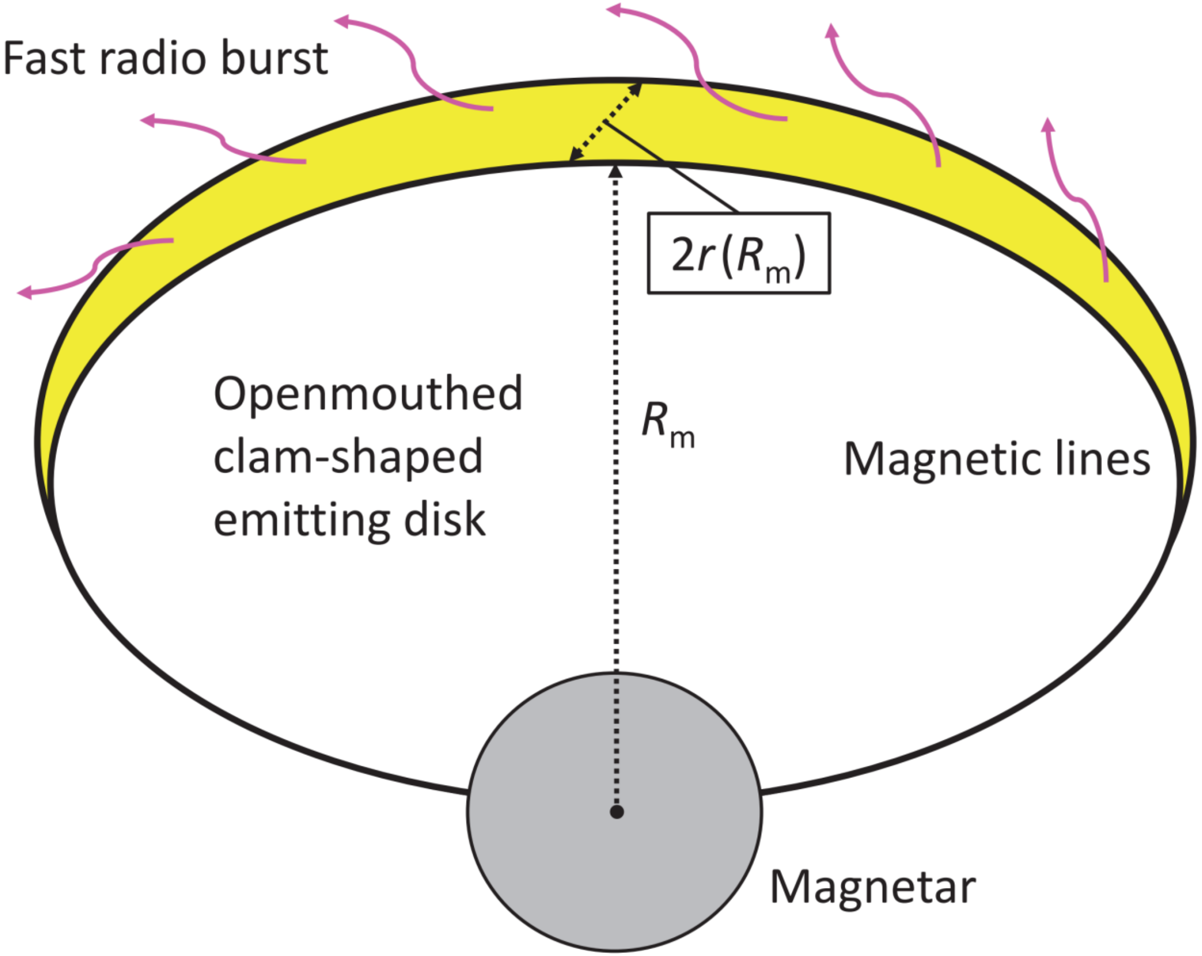

$$\theta_\mathrm{i} \simeq \frac{r(R_\mathrm{m})}{R_\mathrm{m}} \simeq 1.7\times10^{-3}\left(\frac{\Delta t}{0.6\,\mathrm{ms}}\right)^{19/36}\left(\frac{M}{1.4M_\odot}\right)^{15/108}\left(\frac{\mu}{2.2\times10^{32}\,\mathrm{G\,cm^3}}\right)^{-2/9}$$

Features of an FRB/XRB

FRB

The Lorentz factor of electrons accelerated at *R*$_{\mathrm{m}}$ (Dai 2020):

$$\gamma \equiv \chi\gamma_{\max} \simeq \chi\left(\frac{6\pi e|E_2|}{\sigma_T B^2}\right)^{1/2}$$

$$\simeq 140\chi\left(\frac{\Delta t}{0.6\,\mathrm{ms}}\right)^{-5/72}\left(\frac{M}{1.4M_\odot}\right)^{-7/72}\left(\frac{\mu}{2.2\times10^{32}\,\mathrm{G\,cm^3}}\right)^{1/18}$$

The characteristic frequency of their coherent curvature radiation:

$$\nu_{\mathrm{curv}} \simeq 2.0\chi^3\delta\left(\frac{\Delta t}{0.6\,\mathrm{ms}}\right)^{-5/24}\left(\frac{M}{1.4M_\odot}\right)^{-7/24}\left(\frac{\mu}{2.2\times10^{32}\,\mathrm{G\,cm^3}}\right)^{1/6}\left(\frac{\rho_{\mathrm{c}}}{10^7\,\mathrm{cm}}\right)^{-1}\,\mathrm{GHz}$$

$$\simeq 2.5\chi^3\delta\left(\frac{\Delta t}{0.6\,\mathrm{ms}}\right)^{-11/72}\left(\frac{M}{1.4M_\odot}\right)^{-1/72}\left(\frac{\mu}{2.2\times10^{32}\,\mathrm{G\,cm^3}}\right)^{-5/18}\,\mathrm{GHz}$$

where $\delta = 1/\{2\gamma^2[1-\beta\cos(\theta_{\mathrm{v}}-\theta_{\mathrm{i}})]\}$ and $\rho_{\mathrm{c}} = 0.635R_{\mathrm{m}}$

The total luminosity (L_{tot}) of a resultant beamed FRB (Dai 2020):

$$L_{\rm tot} \sim 2.0\times10^{36}\frac{1}{\chi^3}\left(\frac{m}{10^{17}\,{\rm g}}\right)^{8/9}\left(\frac{M}{1.4M_\odot}\right)^{19/12} \times\left(\frac{\mu}{2.2\times10^{32}\,{\rm G\,cm^3}}\right)^{3/2}\left(\frac{R_{\rm m}}{10^7\,{\rm cm}}\right)^{-23/4}\left(\frac{\rho_{\rm c}}{10^7\,{\rm cm}}\right)^{-1}\ {\rm erg\,s^{-1}}$$

FRB

The isotropic-equivalent energy release of the FRB:

$$E_{\rm radio} \simeq \frac{\delta^3}{f}\times L_{\rm tot}\times\Delta t \qquad \text{where}\quad f\equiv\Delta\Omega/(4\pi)\simeq 1/(2\gamma)$$

$$E_{\rm radio}\sim 1.4\times10^{35}\frac{\delta^3}{\chi^2}\left(\frac{\Delta t}{0.6\,{\rm ms}}\right)^{119/36}\left(\frac{M}{1.4M_\odot}\right)^{145/36}\left(\frac{\mu}{2.2\times10^{32}\,{\rm G\,cm^3}}\right)^{-13/9}\ {\rm erg}$$

The total asteroid-magnetar gravitational energy available for an XRB:

$$E_{\rm G} \simeq \frac{GMm_{\rm a}}{R_*} \sim 1.9 \times 10^{40} \left(\frac{m_{\rm a}}{10^{20}\,{\rm g}}\right) \left(\frac{M}{1.4M_\odot}\right) \left(\frac{R_*}{10^6\,{\rm cm}}\right)^{-1} {\rm erg}$$

XRB

This energy is released in a timescale (Dai et al. 2016):

$$t_{\rm a} \simeq \frac{12r_{\rm a}}{5} \left(\frac{R_{\rm d}}{GM}\right)^{1/2} \sim 0.1 \left(\frac{m_{\rm a}}{10^{20}\,{\rm g}}\right)^{1/3} \left(\frac{M}{1.4M_\odot}\right)^{-1/3} {\rm s}$$

A fireball is initially trapped by magnetic field lines and thus its temperature:

$$T_{\rm fb} \sim \left(\frac{B^2}{8\pi a}\right)^{1/4} = 1.8 \times 10^{10} \left(\frac{B}{10^{14}\,{\rm G}}\right)^{1/2} {\rm K}$$

⇒ A dense population of e± pairs, driving a relativistic outflow and an XRB.

3. Constraints on model parameters

If $B_{\rm s} = 2.2\times10^{14}$ G, $M = 1.4M_\odot$, and $R_* = 10^6$ cm are adopted, we obtain

$$R_{\rm m} \sim 1.2\times10^{7}\left(\frac{\Delta t}{0.6\,{\rm ms}}\right)^{-1/18}\ {\rm cm}$$

$$r(R_{\rm m}) \sim 2.1\times10^{4}\left(\frac{\Delta t}{0.6\,{\rm ms}}\right)^{17/36}\ {\rm cm}$$

$$\theta_{\rm i} \sim 1.7\times10^{-3}\left(\frac{\Delta t}{0.6\,{\rm ms}}\right)^{19/36}$$

$$\chi \sim 0.85\left(\frac{\Delta t}{0.6\,{\rm ms}}\right)^{199/792}$$

$$\delta \sim 1.0\left(\frac{\Delta t}{0.6\,{\rm ms}}\right)^{-119/198}$$

$$\gamma \sim 120 \text{ for } \Delta t \sim 0.6\,{\rm ms}$$

The energy release of the XRB associated with FRB 200428 (Dai 2020):

$$E_{\mathrm{X}} \sim 1.9 \times 10^{40} \zeta \left(\frac{m_{\mathrm{a}}}{10^{20}\ \mathrm{g}} \right) \mathrm{erg}$$

- As the asteroid collides with the stellar surface, a resultant **hot fireball** has such a high temperature T_{fb} that a dense population of $e^{\pm}$ pairs are inevitably created.
- Thermal X-rays from a photosphere in the relativistically expanding fireball are emitted and thus **superposition of radiation** from different photospheres leads to a multi-temperature BB spectrum of the XRB.
- Collisions between different shells in the fireball could give rise to **nonthermal emission**, similar to internal shocks in GRBs.
- This model can thus explain the observed spectrum and light curve of the XRB.

Ze-Nan Liu et al. 2020, in preparation

Self-consistent interpretation of observations

① FRB 200428: emission frequency, luminosity, and two pulses

② Associated XRB: luminosity, unusual spectrum, and two peaks

③ Non-detection of pulsed emission prior to FRB 200428 by FAST

④ 3-6 ms delay of XRB's peaks with respect to FRB 200428's pulses

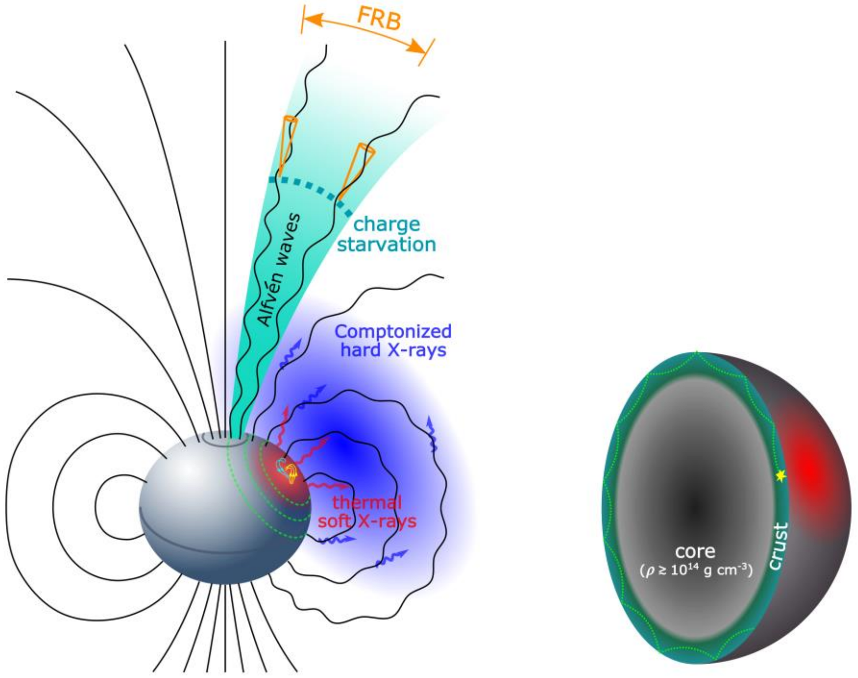

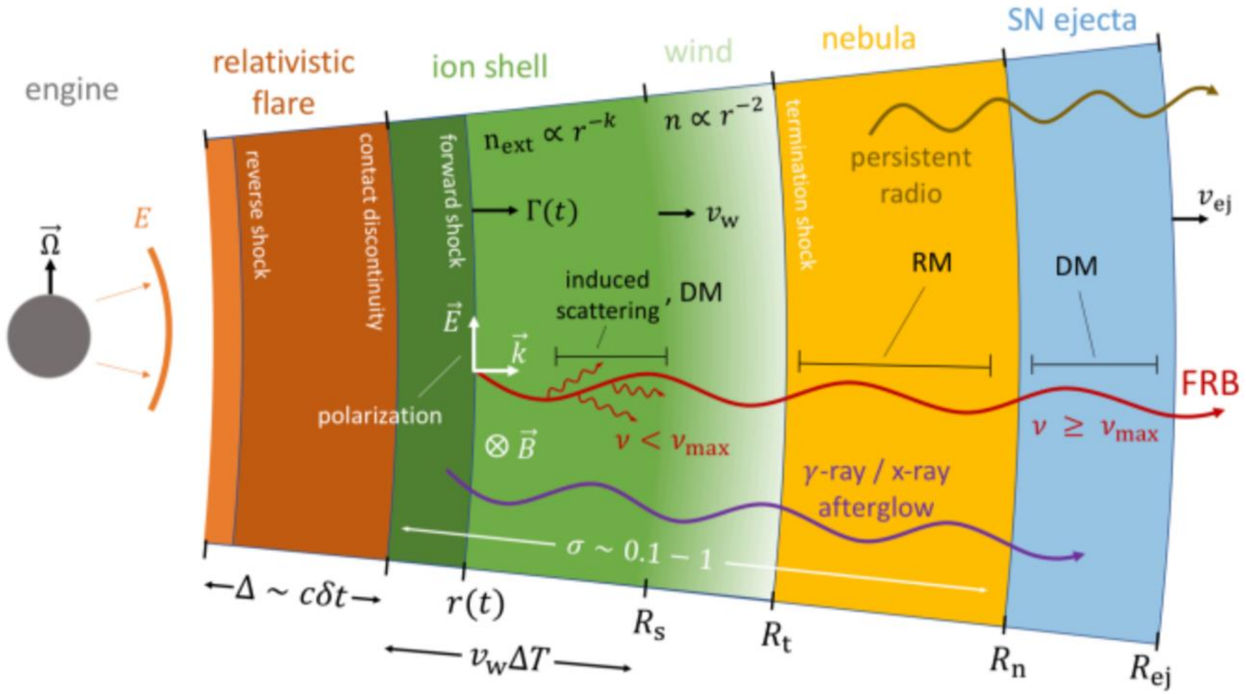

Close-in: Lu et al. 2020 **Far-away:** Margalit et al. 2020; Metzger et al. 2019

⑤ Sites of FRB 200428 and XRB

Δτ = Separation of two pulses of FRB 200428 minus that of XRB

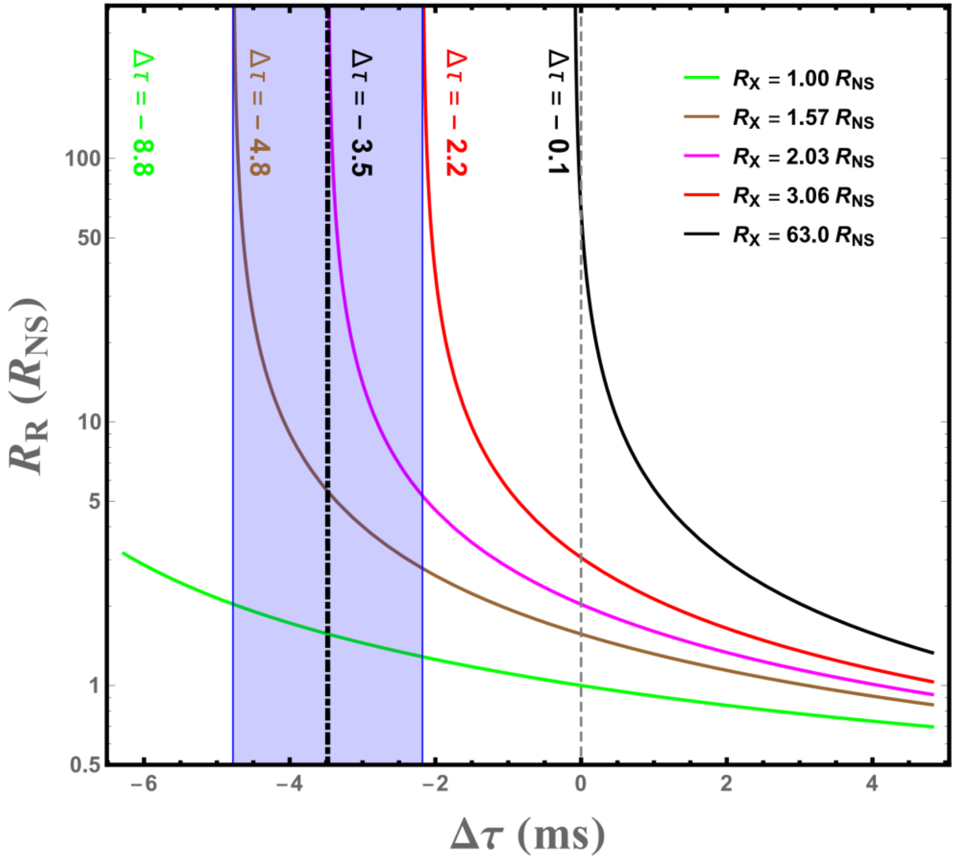

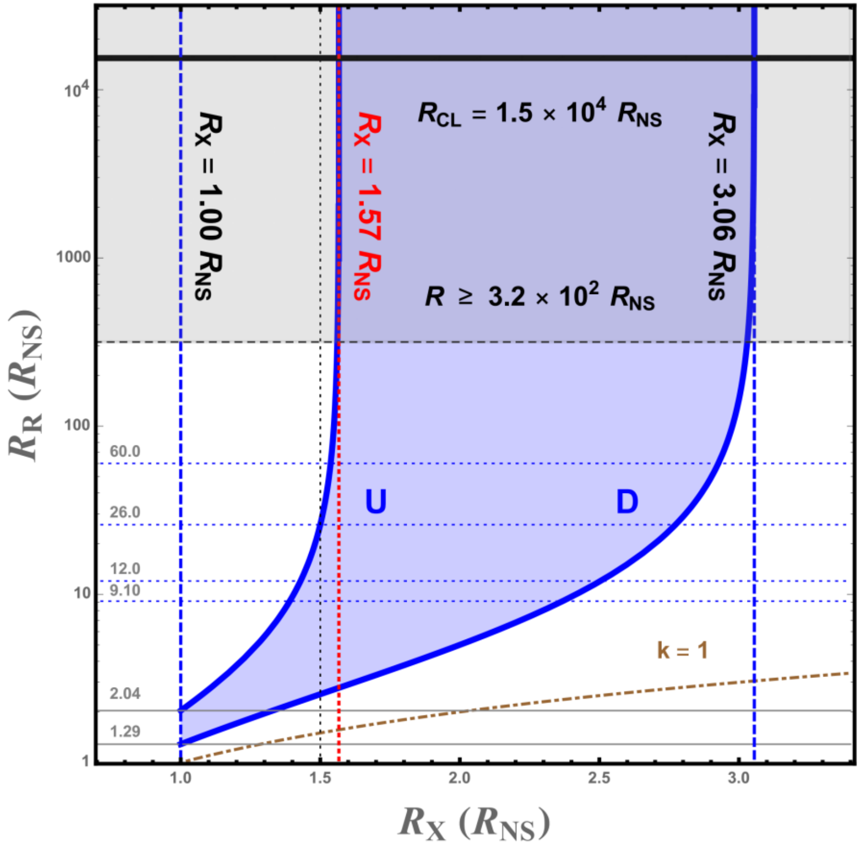

Insight-HXMT:

$\Delta\tau = -3.5 \pm 1.3$ ms

(Zhang et al. 2020)

Gravitational redshift effect

Conclusion:

$R_{FRB} >> R_{NS}$

R_{XRB} ~ a few R_{NS}

⑥ QPO in SGR 1935+2154?

Quasi-periodical flux oscillation of XRB associated with FRB 200428

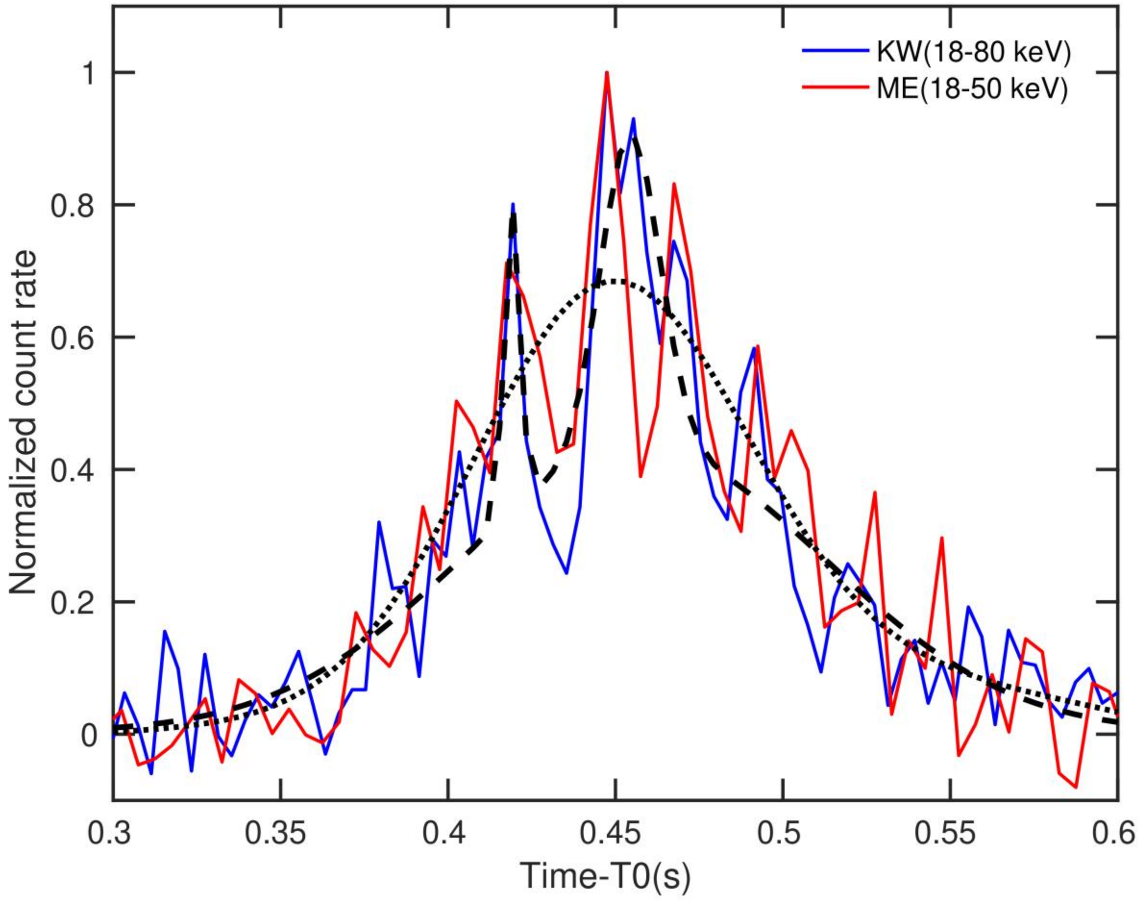

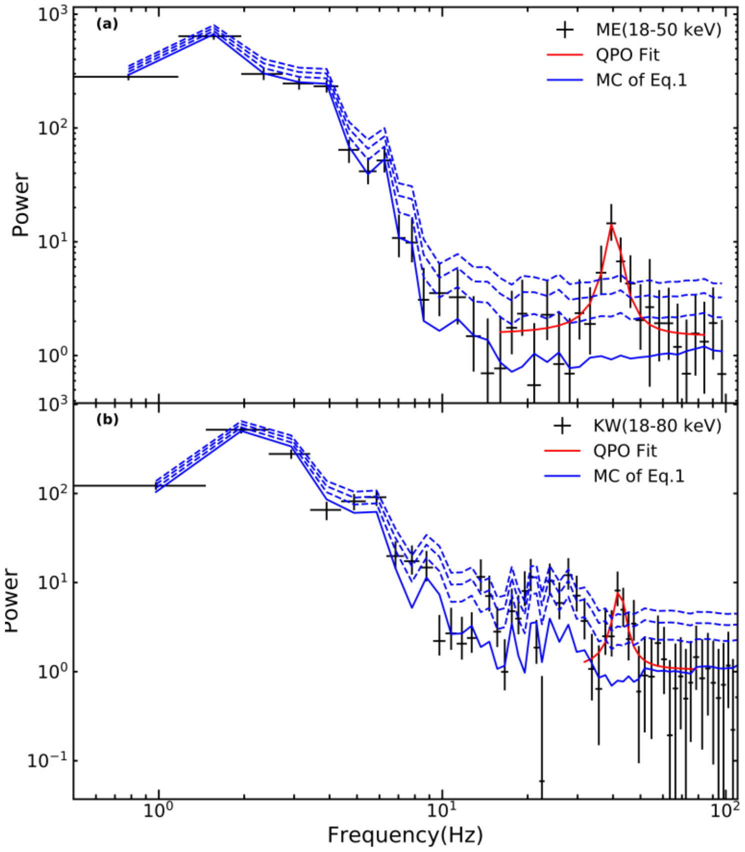

***Insight*-HXMT:**
QPO ν ~ 40 Hz
(Ge et al. 2020)

Initial impact
⇒ crustal oscillation
(Duncan 1998)

4. Conclusions

- **FRB 200428-emitting region for the fragmental mass $m \sim 10^{17}$ g looks like an openmouthed clam, whose inclination angle $\theta_i \sim 1.7\times10^{-3}$.**
- **The typical Lorentz factor of emitting electrons is $\gamma \sim 120$. Our line of sight is just within the solid angle of FRB 200428.**
- **As an asteroid with $m_a \sim 10^{20}$ g collides with the stellar surface, a resultant fireball has a temperature $\sim 2\times10^{10}$ K, leading to $e^{\pm}$ pairs and an XRB.**
- **This model can thus interpret all of the observed features self-consistently.**

“目前似乎只有你的模型还活着”—张双南

Thank you!